The upgraded GMRT: opening new windows on the radio Universe

Y. Gupta, B. Ajithkumar, H. S. Kale, S. Nayak, S. Sabhapathy, S. Sureshkumar, R. V. Swami, J. N. Chengalur, S. K. Ghosh, C. H. Ishwara-Chandra, B. C. Joshi, N. Kanekar, D. V. Lal and S. Roy

The Giant Metrewave Radio Telescope (GMRT) is today a frontline international facility for low-frequency radio astronomy, that has produced several exciting and important new results in the 15 years that it has been operational. To keep the GMRT competitive in the global arena in the future, a major upgrade of the observatory is nearing completion that will increase its sensitivity by up to three times and make it a more powerful and versatile facility. We describe the main goals of this upgrade, highlight the technical features and challenges, outline the science potential, and update the current status of this venture.

Keywords: Radio telescope, upgrade, scientific potential, technical challenges.

Background: motivation and main goals of the GMRT upgrade

The Giant Metrewave Radio Telescope (GMRT) (Swarup et al, 1991; Ananthakrishnan, 1995; Gupta, 2014) is one of the largest and most sensitive fully operational low-frequency radio telescopes in the world today. The array configuration of 30 antennas (each of 45 m diameter) spanning over 25 km, provides a total collecting area of about 30,000 sq. m at metre wavelengths, with a fairly good angular resolution (~arcsec). In addition to the regular earth rotation aperture synthesis mode, the GMRT also provides incoherent and phased array beamformer options (Gupta et al, 2000), which allow for high-quality observations of compact objects like pulsars. Since its commissioning in 2001, the GMRT has produced several new and interesting results in a wide range of topics in astrophysics – see the proceedings of the conference ‘The Metrewavelength Sky’ (Chengalur & Gupta, 2014) for a representative collection of sample results. At present, an average of about 40 papers per year are published in refereed journals that are based fully or in part on data from the GMRT. About 50% of the users of the GMRT are PIs from India, with the rest coming from about 30 different countries (see Gupta, 2014 for details). The oversubscription rate for the GMRT is typically around two or more.

The GMRT was one of the first in a series of new radio observatories that heralded the renaissance of low-frequency radio astronomy in the 1990s. Shortly after its commissioning, new facilities such as LOFAR (e.g. var Haarlem et al, 2013), MWA (e.g. Tingay et al. 2013), LWA (e.g. Ellingson et al, 2013) were conceived and started becoming operational towards the end of the first decade of this century.

Keeping in mind the growth of low-frequency radio astronomy in the world, and learning from our own efforts and experiences of building and using the GMRT, a plan to upgrade the GMRT was proposed during the XI Plan funding period (2007−2012) and the first serious work in this direction was initiated around 2010. The main goal identified was to add extra capability to the existing GMRT array in terms of frequency coverage and sensitivity, which would allow to open new windows of research in astrophysics and the study of the Universe.

More specifically, the improved frequency coverage, to be achieved by broadbanding the receiver systems, would allow spectral line observations over a wider range of the centimetre and metre wavelength spectrum, allowing for explorations of the Universe over a much wider range of redshifts than is possible with the existing GMRT. The increased sensitivity, to be achieved by a combination of wider bandwidths and improved technology receivers, would improve the capability of the GMRT for continuum imaging, allowing many more refined galactic and extra-galactic studies to be carried out, and also make it a more powerful tool for detection and detailed studies of pulsars and transients.

With the above-stated objectives in mind, the following were identified as the main targets for the upgraded GMRT (uGMRT): (1) Seamless frequency coverage, as far as possible, from 50 to 1500 MHz, replacing the five limited bandwidth frequency bands of the original GMRT design. (2) Maximum instantaneous bandwidth of 400 MHz, instead of the 32 MHz bandwidth of the original GMRT design. (3) Improved receiver systems with

*For correspondence. (e-mail:

higher G/T_{sys} and better dynamic range. (4) Versatile digital backend correlator and pulsar receiver catering to the 400 MHz bandwidth. (5) Revamped, modern servo system. (6) Sophisticated, next-generation monitor and control system. (7) Matching improvements in mechanical systems, electrical and civil infrastructure and computing resources. (8) Implementation of the upgrade with minimal disruption to the availability of the existing GMRT for scientific observations.

Implementation of the upgrade and challenges faced

The seamless frequency coverage alongwith wide bandwidths have been achieved by the design of feeds and frontend electronics in octave ranges of frequency, followed by an improved wideband optical fibre transmission scheme to transport the radio frequency (RF) signals from the antennas to the central receiver building (Sureshkumar, 2014), and wide bandwidth analog and digital backends at the central receiver building (Ajithkumar, 2014). The final choice of bands for the uGMRT is: 50−80 MHz (band-1), 120–250 MHz (band-2), 250–500 MHz (band-3), 550–850 MHz (band-4), 1050–1450 MHz (band-5). Among these five bands, the last four have been chosen for implementation and commissioning in the first phase of the uGMRT, and the design and implementation of band-1 has been deferred for the present. The gaps in the frequency coverage in this choice of bands is due to constraints of very strong radio frequency interference (RFI) such as the FM band, TV channels and mobile communication bands (other sources of RFI which occur within the selected bands have been mitigated using different schemes as described below). Figure 1 shows the frequency coverage targetted with the uGMRT, alongwith the fractional bandwidth for each receiver band.

Frontend and optical fibre systems

The frontend receiver for each band consists of a wideband dual polarization feed at the focus of the GMRT antenna; followed by a polarizer (for all bands, except band-5) that converts linear polarization signals to circular, matching, low-noise amplifiers and then appropriate band-limiting filters (with special notch filters for rejecting RFI where needed). This is followed by a common set of electronics (the ‘common box’) where the two signals from the desired band are selected, a phase switcher for Walsh modulation is available as an option, and the signals are amplified to the final desired level before being transmitted from the focus down to the base of the antenna (Sureshkumar, 2014). For the 1050–1450 MHz band-5 system, the existing broadband feed (900–1450 MHz) has been coupled with an improved version of the existing frontend system with better dynamic range and improved rejection of the strong RFI from the mobile phone band (850–1050 MHz). For band-2, band-3 and band-4, the design of new wideband feeds with matching improved frontend electronics posed significant challenges, which have been met successfully by the GMRT team (e.g. Bhandari et al, 2013; Raut et al, 2013; Chatterjee et al, 2015). The overall upgraded GMRT frontend chain provides wideband frequency coverage with improved dynamic range (6–10 dB for most of the bands) and better filtering of RFI signals.

At the antenna base, the incoming RF signal for each polarization is split into two copies, one of which goes to the existing legacy GMRT receiver system, and the other goes to the wideband uGMRT receiver system. The final signals from these two paths are modulated onto different wavelengths (using separate lasers) and transmitted over the same optical fibre to the central receiver building, thereby making it possible to meet the important requirement of simultaneous operation of both legacy and upgraded GMRT systems (Sureshkumar, 2014). The upgraded optical fibre link also supports a bidirectional 1 Gbit ethernet link for supporting the new monitor and control system being designed for the uGMRT. At the central receiver building, optical signals from both the legacy and upgraded GMRT systems are converted back to electrical voltages and processed separately in parallel.

Analog and digital backend systems

For the uGMRT, the wideband RF signals from the output of the optical fibre system are first sent to the uGMRT analog backend system which converts them down to baseband signals of 100, 200 or 400 MHz bandwidth with a single-step direct conversion scheme using broadband frequency mixer circuits where the local oscillators are locked to the frequency reference signal of the observatory (Ajithkumar, 2014). The 30-antenna dual polarization baseband signals with maximum bandwidth of 400 MHz are then sent to the uGMRT digital backend system that first digitizes the signals and then processes them using a hybrid FPGA + GPU-based distributed computing design, to implement a full polar correlator and a beam former with up to four incoherent or coherent array beams, working for up to 16,384 spectral channels across the band (Reddy et al, 2017; Ajithkumar, 2014, 2013). It also has narrow-bandwidth zoom modes for spectral line observations. Further, it has facilities for real-time filtering of RFI signals (both narrow-band spectral RFI and wideband impulsive RFI) at different stages of the processing (e.g. Buch et al, 2016), and a capability for Walsh demodulation (Chaudhari et al, 2017).

The final outputs from the correlator and beam former are available in the form of data files recorded on disk, that go through off-line processing to produce the final images and other products. Unlike the legacy GMRT system, the uGMRT does not have an automatic-level control circuity to maintain constant signal power level into the backend system. This is instead achieved by a power equalization scheme designed to operate on a software-based approach, with full control by the users.

Monitor and control, servo, mechanical and electrical systems

The upgrade aims to equip the GMRT with a next-generation monitor and control (M&C) system (Kodilkar et al, 2013; Nayak, 2014). At the hardware level, this involves replacement of the existing M&C hardware controller cards and network with modern micro-controllers connected to the main control computer via ethernet links to each antenna. At the software level, it involves a change-over of the existing high-level M&C 'on-line' software to a next-generation software that follows modern architectural principles. This has direct synergy with the Indian contribution to the design of the Telescope Manager System for the SKA, with the uGMRT developments aimed as acting as a pathfinder for the SKA effort. Care has been taken to meet the challenge of being able to operate the GMRT with full support for simultaneous observations with the legacy GMRT and the upgraded GMRT systems.

As part of the RFI mitigation exercise, a new feature has been added to the GMRT, i.e. a scheme for real-time monitoring of the presently known man-made satellites that affect the uGMRT bands, and generating warning signals in the control room whenever the antennas come within a pre-determined zone of avoidance of any satellite in the sky (Raybole et al., 2016). Further, these warnings can be generated a priori for any observation planned in the near future, and a posteriori for observations done in the past. This scheme is now available for the uGMRT on a routine basis, and holds great promise for mitigating the challenge of RFI from satellite transmissions.

The legacy servo control system for the GMRT has gone through a major revamp, driven by the needs for improved reliability, mitigating against obsolescence, as well as improved performance and capabilities (e.g. Bagde, 2014). Significant aspects related to maintenance and improvements of the mechanical structure of the GMRT antennas have been taken up as part of the upgrade exercise (e.g. Nandi, 2014), with management of corrosion-related effects being the biggest challenge here. For the electrical systems, upgrade activities include improvements at the antennas such as RFI-friendly UPS units, diesel generator back-up arrangements for the entire array, and improvements at the central receiver building such as higher capacity modular UPS units.

System parameters and targeted sensitivity of the uGMRT

Based on the above described design of the GMRT upgrade, the main system parameters expected for the uGMRT are summarized in Table 1. As can be seen, the uGMRT can, in the ideal situation, achieve sub-mJy sensitivities for imaging and detection of pulsars in 10 min of observing time.

Figure 2 compares the targetted sensitivity of the uGMRT vis-a-vis other global facilities already in operation (or in the planning stages), for a typical full-synthesis continuum mode observation. As can be seen, the uGMRT will be one of the most sensitive facilities in the frequency range 250–1500 MHz till the SKA Phase-1, with its currently planned specifications, is commissioned. Furthermore, as can be seen from the dashed lines in Figure 2 (which indicate the flux density of a typical extra-galactic source with power-law behaviour, $S_\nu \propto \nu^\alpha$ and spectral index $\alpha = -0.7$), the uGMRT at 300–1000 MHz will be well matched to (or better than) the JVLA at higher frequencies (3–10 GHz), thereby providing a powerful combination for exploring a wide range of astrophysical phenomena.

Scientific potential of the upgrade

The uGMRT, with the increased frequency coverage, wider bandwidths and improved receiver systems, offers significant potential for new science covering diverse areas. Given that the uGMRT will be one of the most sensitive instruments operating at centimetre and decimetre wavelengths till SKA Phase-1 is ready, many of the science projects with the uGMRT will probe new regimes. Here we highlight the possibilities, alongwith some sample results.

Spectral line science

The increased frequency coverage of the uGMRT offers outstanding near-seamless redshift coverage in the spectral lines of neutral hydrogen (Hi 21 cm; $z \approx 0$–10) and hydroxyl (OH 18 cm; $z \approx 0.16$–12). This would allow searches for redshifted Hi 21 cm absorption from damped Lyman-α absorbers (DLAs) and neutral hydrogen associated with active galactic nuclei (AGNs) out to the highest redshifts at which these systems have been discovered, allowing one to probe the redshift evolution of DLA spin temperatures, and the presence and kinematics of neutral gas in AGN environments (e.g. Morganti et al. 2015). Indeed, the first uGMRT observations of DLAs have already detected redshifted Hi 21 cm absorption in two high-z galaxies (Kanekar 2014; Figure 3). The wide bandwidth and excellent spectral resolution of the GWB will enable measurements of the average gas mass of galaxies and the cosmological gas mass density out to $z \approx 1.5$, via 'stacking' of the Hi 21 cm emission lines from galaxies with known redshifts in optical deep fields (e.g. Kanekar et al. 2016). Detections of OH 1667 MHz megamaser emission from hyperluminous infrared galaxies and lensed ultraluminous infrared galaxies should be possible out to $z \approx 3$, allowing one to probe physical conditions in massive starburst galaxies (e.g. Darling and Giovanelli 2002).

The wide frequency coverage will also allow 'blind' surveys for atomic and molecular absorption at high redshifts, which should yield the detection of new absorbers that might be used to study redshift evolution in the fundamental constants of physics (e.g. Chengalur & Kanekar 2003). The new frequency coverage will also provide access to new molecular transitions (e.g. CH at ≈ 701 MHz and CH_3OH at 834 MHz) that have not so far been observable with interferometers, allowing one to probe the large-scale spatial structure of molecular clouds in the galaxy (e.g. Chengalur and Kanekar 2003). Finally, the significantly higher spectral resolution offered by the GWB also makes the uGMRT a superb instrument for deep, high-velocity resolution absorption studies of the galactic interstellar medium, as would be needed to study the properties of atomic gas in the warm or unstable phases of the ISM (e.g. Heiles & Troland 2003; Roy et al. 2013).

Continuum imaging science

The improved sensitivity for continuum imaging with large bandwidths has great potential for new science with the uGMRT. Mapping of diffuse, extended, low-surface brightness emission requires a good sampling of the *u–v* plane to image the emission over a large range of angular scales (e.g. Feretti et al, 2012). The large fractional bandwidths of the uGMRT bands (Figure 1) provide excellent *u–v* coverage to map such diffuse structures. This, together with the improved sensitivity and arcsecond-scale resolution (see Figure 4 for a sample result) will open up several areas of study: (i) revealing new features in clusters and groups of galaxies at MHz frequencies for the first time (e.g. Gendron-Marsolais et al, 2017; Kale et al, 2016); (ii) studying interesting radio galaxies, from low luminosity AGNs in the nearby Universe to powerful radio galaxies at high redshifts, along with their spectral structure in detail at low radio frequencies (e.g. Lal & Rao, 2007; Kharb et al, 2016); (iii) discovering MHz peaked spectrum (MPS) sources, which are possibly GHz peaked spectrum (GPS) source populations at high redshifts ($z \sim 3$) (e.g. Callingham et al, 2017); (iv) searching for steep-spectrum radio sources which are strong candidates for high redshift radio galaxies (e.g. Ishwar-Chandra et al, 2010); (v) detecting weak radio emission from galaxies, thereby allowing to infer the propagation of older cosmic ray electrons generated in galaxies (e.g. Beswick et al, 2015); (vi) estimating frequency break in the spectra of electron populations emitting synchrotron emission, e.g. steep spectrum relic and halo sources, supernova events, GRB events, etc. (e.g. Chandra, Ray & Bhatnagar, 2004); (vii) separating thermal vs non-thermal sources in the galactic plane while imaging with the large bandwidths (e.g. Prandoni & Seymour, 2015); (viii) enhanced ability to detect transient sources of various kinds, as has been demonstrated with the legacy GMRT system and other facilities (e.g. Roy et al, 2010; Chandra et al, 2016).

In addition to the above specific kinds of objects and science topics, one area where the GMRT has made a difference and the uGMRT is expected to excel further, is that of low-frequency all-sky surveys. The 150 MHz survey TGSS carried out with the GMRT (https://tgss.ncra.tifr.res.in and Intema *et al*., 2016), providing a sensitivity complementary to that of the NVSS at 1400 MHz (assuming the typical spectral index of –0.7, as in figure 2), is already proving useful. With the wider bands of the uGMRT, like the 250–500 MHz band-3, an all-sky survey can be carried out that will be more than an order of magnitude deeper than the TGSS with four times higher resolution, which will be complementary to other contemporary surveys, planned or on-going, such as the VLASS (at higher frequencies) and the LOFAR Tier-1 survey (at lower frequencies).

Pulsar science

As pulsars are steep spectrum sources, sensitive observations of these objects are well motivated in the 150–1500 MHz frequency range, where the uGMRT will open new possibilities with its wide frequency coverage and improved sensitivity. Figure 5 shows a sample of the improved sensitivity, from the early commissioning tests of the beamformer mode of the GWB receiver. The wideband coverage in band-3 and band-4 should make possible highly sensitive pulsar surveys which should be a natural follow-up to the recent and ongoing efforts with the legacy GMRT system (e.g. Joshi et al, 2009; Bhattacharyya et al, 2016). Targetted searches (and their follow-up), which have enjoyed good success with the legacy GMRT (e.g. Freire et al, 2004; Gupta et al, 2005; Roy, Gupta & Lewandowski, 2012; Bhattacharyya et al, 2013) would also become much more rewarding exercises with the uGMRT.

The higher sensitivity will also improve the capabilities for interesting studies of pulsar emission properties that have been attempted with the legacy GMRT system (e.g. Gangadhara & Gupta, 2001; Bhattacharyya et al, 2007; Kijak et al, 2011; Basu, Mitra & Athreya, 2011; Gajjar, Joshi & Kramer, 2012; Mitra et al, 2016; De, Gupta & Sharma, 2016). This, coupled with the ability to observe simultaneously at different bands of the uGMRT using the subarray capability and multiple beams provided by the upgraded 400 MHz digital backend, will enhance the power of the GMRT to carry out multi-frequency studies of pulsars. Such observations are important for (a) precision timing experiments, such as pulsar timing arrays (e.g. Verbiest et al, 2016), specifically to be able to track changes in dispersion measure (e.g. Lam et al, 2016; Kumar et al, 2012); (b) improving our understanding of the pulsar emission mechanism using simultaneous multi-frequency single-pulse observations (e.g. Kramer et al, 2003; Bhat et al, 2007).

Current status and summary

As the upgrade has progressed in an incremental manner, the uGMRT with gradually increasing capabilities has been released for use to the global community, starting with a shared risk mode and maturing to a formal release mode. This has allowed the engineering teams to space out the efforts for mass production, allowed a phased testing of the different upgrade systems to be carried out, and also allowed users to get a feel for the capabilities and quality of the upgraded systems before launching full-scale projects with the uGMRT.

The next major release is planned for October 2017 with two wideband systems (band-3 and band-5) fully equipped on 30 antennas, and a third system (band-4) available on 24+ antennas, alongwith a full correlator and beamformer that can process the maximum bandwidth of 400 MHz. The work on band-2 is progressing apace, alongwith other activities of the upgrade, and the full uGMRT capability is expected to be available to the users by April 2018. Already, interesting new results have begun to be published using the uGMRT capabilities, and many more are expected in the near future.

In summary, the upgraded GMRT, which promises to open exciting new windows on the low-frequency radio Universe, has crossed the major design stages and is well on its way towards becoming a facility that will be available to the global astronomy community.

1. Swarup, G. *et al.*, *Curr. Sci.*, 1991, **60**, 95.
2. Ananthakrishnan, S., *J. Astrophys. Astron.*, 1995, **16**, 427.
3. Gupta, Y., In *The Metrewavelength Sky* (eds Chengalur, J. N. and Gupta, Y.), *ASI Conference Series*, 2014, **13**, 197.
4. Gupta Y. *et al.*, In *Pulsar Astronomy – 2000 and Beyond*, IAU Colloq. 2000, **177**, 202, 277.
5. Chengalur, J. N. and Gupta, Y. (eds), *The Metrewavelength Sky*, ASI Conference Series, 2014, Vol. 13.
6. van Haarlem, M. P. *et al.*, *A&A*, 2013, **556**, A2.
7. Tingay, S. *et al.*, *PASA*, 2013, **30**, e007.
8. Ellingson, S. W. *et al.*, *IEEE Trans. Antennas Propag.*, 2013.
9. Sureshkumar, S., In *The Metrewavelength Sky* (eds Chengalur, J. N. and Gupta, Y.), ASI Conference Series, 2014, vol. 13, p. 197.
10. Bhandari, H. R., Sankarasubramanian, G. and Praveen Kumar, A., In IOP Conference Series: Material Science and Engineering, 2013, **44**, 012025.
11. Raut, A., Bhalerao, V. and Praveen Kumar, A., In IOP Conf. Series: Material Science and Engineering, 2013, **44**, 012025.
12. Chatterjee, S., Raut, A. and Sureshkumar, S., In IEEE Aerospace and Electronics System, 2015, **30**(3).
13. Ajithkumar, B., In *The Metrewavelength Sky* (eds Chengalur, J. N. and Gupta, Y.), ASI Conference Series, 2014, vol. 13, p. 197.
14. Reddy, S. H. *et al.*, *J. Astron. Instrum.*, 2017, **6**(1), 164011.
15. Ajithkumar, B. *et al.*, In IOP Conference Series : Material Science and Engineering, 2013, vol. 44, 012025.
16. Buch, K. D. *et al.*, *J. Astron. Instrum.*, 2016, **5**(4), 1641018.
17. Chaudhari, S. C. *et al.*, *J. Astron. Instrum.*, 2017, **6**(1), 164017.
18. Kodilkar, J. P. *et al.*, In IOP Conference Series: Material Science and Engineering, 2013, vol. 44, 012025.
19. Nayak, S., In *The Metrewavelength Sky* (eds Chengalur, J. N. and Gupta, Y.), ASI Conference Series, 2014, vol. 13, p. 197.
20. Bagde, S. K., In *The Metrewavelength Sky* (eds Chengalur, J. N. and Gupta, Y.), ASI Conference Series, 2014, vol. 13, p. 197.
21. Nandi, A. K., In The Metrewavelength Sky (eds Chengalur, J. N. and Gupta, Y.), ASI Conference Series, 2014, vol. 13, p. 197.
22. Morganti, R., Sadler, E. M. and Curran, S. J., In Advancing Astrophysics with the Square Kilometre Array, arxiv:1501.01091, 2015.
23. Kanekar, N., *ApJL*, 2014, **797**, L20.
24. Kanekar, N., Sethi, S. and Dwarakanath, K. S., *ApJL*, 2016, **818**, L28.
25. Darling, J. and Giovanelli, R., *AJ*, 2002, **124**, 100.
26. Chengalur, J. N. and Kanekar, N., *Phys. Rev. Lett.*, 2003, **91**, 241302.
27. Chengalur, J. N. and Kanekar, N., *A&A*, 2003, **403**, L43.
28. Heiles, C. and Troland, T., *ApJ*, 2003, **586**, 1067.
29. Roy, N., Kanekar, N., Braun, R. and Chengalur, J. N., *MNRAS*, 2013, **436**, 2366.
30. Feretti, L. *et al.*, AARv, 2012, **20**, 54.
31. Gendron-Marsolais, M. *et al.*, 2017, in press, 2017arXiv:1701.03791.
32. Kale, R. *et al.*, *J. Astrophys. Astron.*, 2016, **37**, 31.
33. Lal, D. V. and Rao, A. P., *MNRAS*, 2007, **374**, 1085.
34. Kharb, P. *et al.*, *J. Astrophys. Astron*., 2016, **37**, 34.
35. Callingham. J. R. *et al.*, *ApJ*, 2017, in press, arXiv:1701.02771.
36. Ishwara-Chandra C. H. *et al.*, *MNRAS*, 2010, **405**, 436.
37. Beswick R. J. *et al.*, In Advancing Astrophysics with the Square Kilometre Array (AASKA14), 2015, p. 1041.
38. Chandra, P., Ray, A. and Bhatnagar, S., *ApJ*, 2004, **612**, 974.
39. Prandoni I. and Seymour, N., In ‘Advancing Astrophysics with the Square Kilometre Array (AASKA14), 2015, 991.
40. Roy, S. *et al.*, *ApJL*, 2010, **712**, L5.
41. Chandra, P. *et al.*, *J. Astrophys. Astron*., 2016, **37**, 30.
42. Intema, H. T., Jagannathan, P., Mooley, K. P. and Frail, D. A., *A&A*, 2017, in press (arXiv:1603.04368).
43. Bhattacharyya, B. *et al.*, *ApJ*, 2016, **817**, 130.
44. Joshi, B. C. *et al.*, *MNRAS*, 2009, **398**, 943.
45. Freire, P. C., Gupta, Y., Ransom, S. M. and Ishwara-Chandra, C. H., *ApJL*, 2004, **606**, L53.
46. Gupta, Y., Mitra, D., Green, D. A. and Acharyya, A., *Curr. Sci.*, 2005, **89**, 853.
47. Roy, J., Gupta, Y. and Lewandowski, W., *MNRAS*, 2012, **424**, 2213.
48. Bhattacharyya, B. *et al.*, *ApJL*, 2013, **773**, L12.
49. Gangadhara, R. T. and Gupta, Y., *ApJ*, 2003, **584**, 418.
50. Bhattacharyya, B. *et al.*, *MNRAS*, 2007, **377**, L10.
51. Basu, R., Athreya, R. and Mitra, D., *ApJ*, 2011, **728**, 157.
52. Gajjar, V., Joshi, B. C. and Kramer, M., *MNRAS*, 2012, **424**, 1197.
53. Mitra, D. *et al.*, 2016, *ApJ*, 833, 28.
54. De, K., Gupta, Y. and Sharma, P., *ApJL*, 2016, **833**, 10.
55. Verbiest, J. P. W. *et al.*, *MNRAS*, 2016, **458**, 1267.
56. Lam, M. T. *et al.*, *ApJ*, 2016, **821**, 66.

57. Kumar, U. *et al.*, In *Proceedings of IAU Symposium 291* (ed. van Leeuwen, J.), 2012.
58. Kramer, M. *et al.*, *A&A*, 2003, **407**, 655.
59. Bhat, N. D. R. *et al.*, *A&A*, 2007, **462**, 257.
60. Sureshkumar, S. *et al.*, In 'Coexisting with Radio Frequency Interference (RFI2016), published by IEEE, 2016, p. 123.
61. Raybole, P. A. *et al.*, In *Coexisting with Radio Frequency Interference (RFI2016)*, published by IEEE, p. 96, 2016.

ACKNOWLEDGEMENTS. A large team of engineers, technical staff and scientists has worked to build the uGMRT, and it is a pleasure to acknowledge the contributions of all members (too numerous to name individually).

doi:

Table 1. System parameters of the uGMRT

	Frequency (f, MHz)			
	Band 2	Band 3	Band 4	Band 5
Frequency range (MHz)	120–250	250–500	550–850	1050–1450
Total system temperature (K)	760–200	165–100	105–100	80–75
Primary beam (arc min)	152*(185/f)	70*(375/f)	37*(700/f)	27*(1250/f)
Antenna gain (K/Jy/antenna)	0.33	0.38	0.35	0.28–0.22
Synthesized beam (arcsec):				
Whole array	17*(185/f)	8*(375/f)	4*(700/f)	2*(1250/f)
Central square	343*(185/f)	174*(375/f)	87*(700/f)	45*(1400/f)
Sensitivity				
RMS noise in image (μJy)*,**	190	50	40	45
Incoherent array sensitivity (μJy)*,***,****	1500	300	220	200

*For 30 antennas and average T_{sys} over the band; **For 10 min integration and 100 MHz bandwidth; ***For 10 min integration and full bandwidth. ****Minimum detectable pulsar flux for long-period pulsars (5σ).

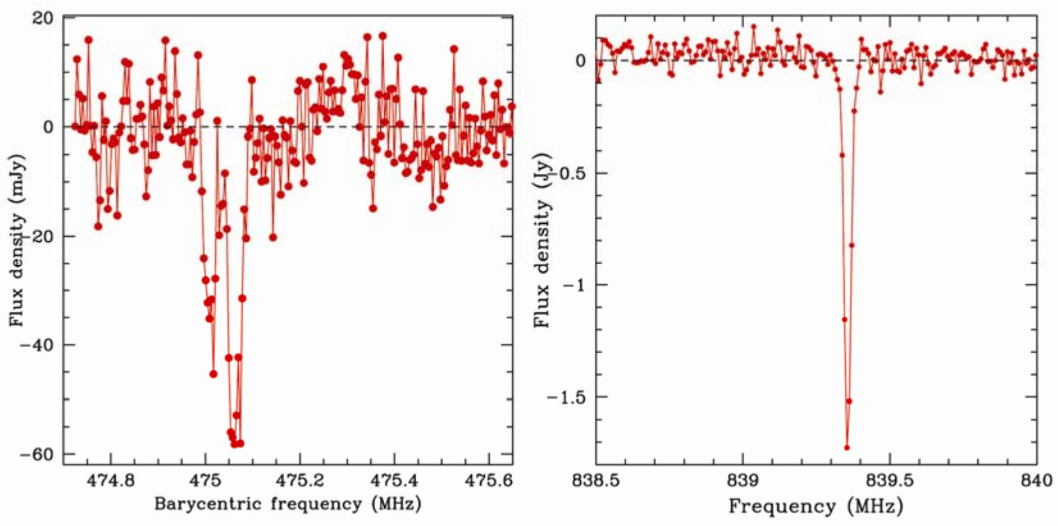

Figure 3. Detections of redshifted Hi 21 cm absorption with the new band-3 and band-4 uGMRT receivers. (Left panel): The $z = 1.9888$ DLA towards 1850 + 402 (Kanekar 2014). (Right panel): The $z = 0.69215$ DLA towards 3C286.

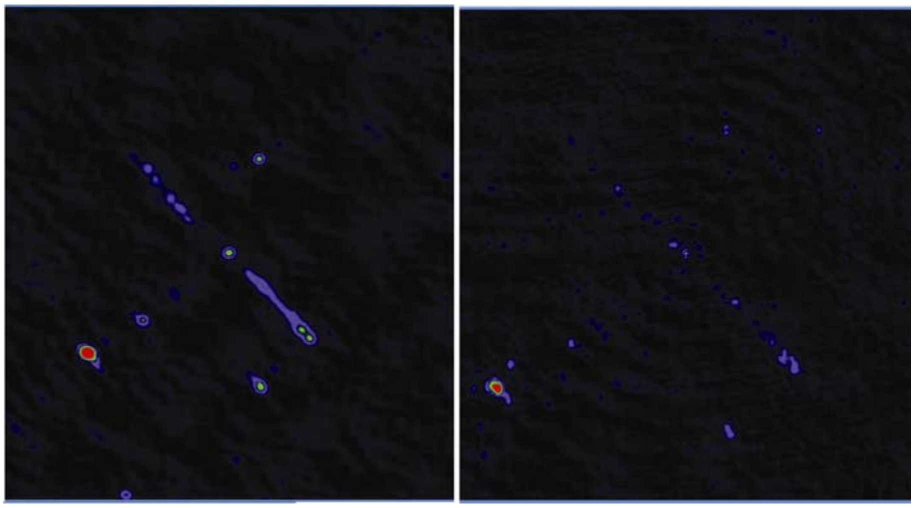

Figure 4. Comparison of sample continuum imaging results at the L-band from the uGMRT system (using 250 MHz bandwidth of band-5 and only 2 h of integration time; left panel) with the legacy GMRT system (using 14 MHz bandwidth and 4 h of integration time; right panel), using the same set of antennas, for a giant radio source illustrating the improved quality of the imaging in terms of lower rms noise (35 vs 50 μJy) and reduced artefacts.

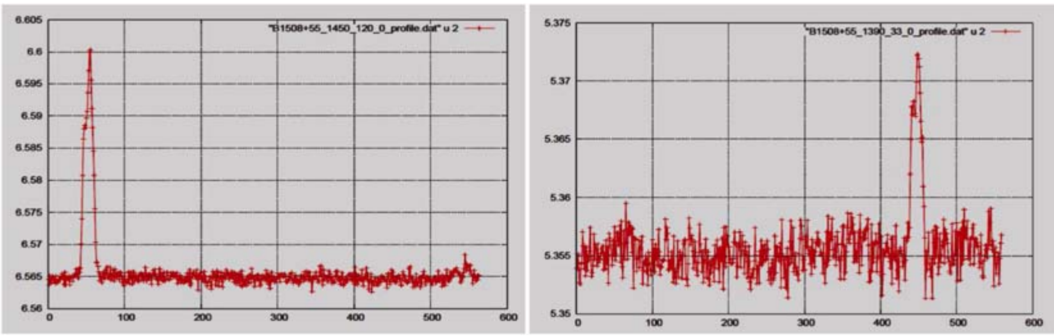

Figure 5. Comparison of sample pulsar observations at the L-band from the uGMRT system (using 200 MHz bandwidth of band-5; left panel) with the legacy GMRT system (using 32 MHz bandwidth; right panel) for PSR B1508 + 55, carried out simultaneously with the same set of eight antennas for 10 min, illustrating the improved sensitivity of the uGMRT system.

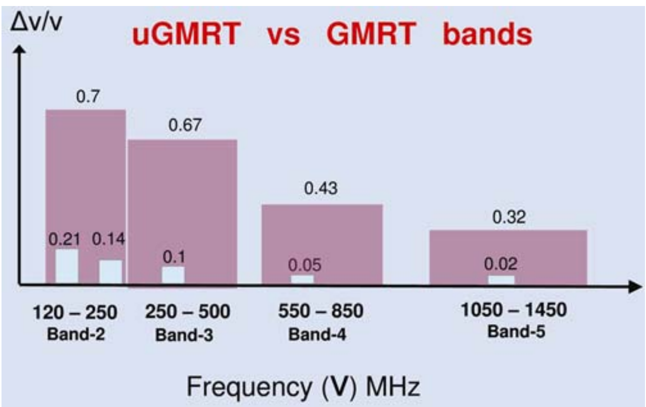

Figure 1. Frequency coverage and fractional bandwidth of the four uGMRT bands being commissioned at present, in comparison with the existing GMRT bands (figure courtesy: Ruta Kale, NCRA).

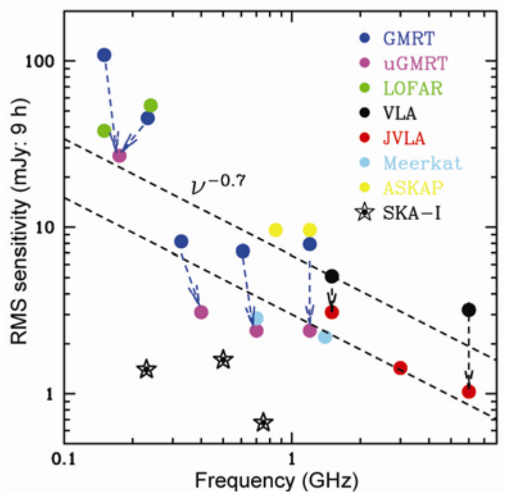

Figure 2. Comparison between the continuum sensitivities of existing and upcoming radio interferometers, for a 9 h on-source integration. The points show the sensitivities of GMRT, VLA, JVLA, uGMRT, LOFAR, MeerKAT, ASKAP and SKA-1-Mid in the colours and symbols as indicated in the key, for different parts of the spectrum in which these facilities operate (see text for more details). As can be seen, uGMRT will be the most sensitive interferometer in the world at frequencies 250–1500 MHz until the advent of Phase-1 of the SKA.